Z. Flugwiss. Weltraumforsch. 19 (1995) 29–33 © Springer-Verlag 1995

Experimental and numerical investigation of the density field in a supersonic combustor with backward facing steps

W. Gabler, F. Mayinger, R. Hannappel

Summary Experimental and numerical data on the flow structure in supersonic combustion chambers are important for the design of high performance SCRAM jet propulsion systems. This paper concentrates on the investigation of the non-reactive flow field in a supersonic multistep combustor with backward facing steps and fuel injection. The influence of the injected fuel on the flow field in a supersonic combustion chamber was investigated using non-intrusive diagnostic methods. Special interest focused on its impact on the reattachment length of the shear layer and the structure of the oblique shock wave system.

Eddies, that are induced by local velocity gradients in the flow field, are able to enhance the mixing process in supersonic combustion chambers [1]. These gradients are caused by shock waves, expansion fans and free shear layers and induce local density gradients. An Euler code was developed to compute the density and the local Mach number distribution in the flow field in order to get insight into the flow structures that could be seen in the experiments.

Experimentelle und numerische Untersuchung der Dichtestruktur in einer Überschallbrennkammer mit Rücksprüngen

Übersicht Für die Konstruktion und Auslegung von Scram-Jet Antrieben werden experimentelle und numerische Daten bezüglich der Strömungsstruktur in Überschallbrennkammern benötigt. Der hier vorgestellte Beitrag behandelt die Untersuchung von nicht reagierenden Strömungsfeldern in einer Überschallbrennkammer mit einer Kaskade von Rücksprüngen und einer gestaffelten Mehrfacheinblasung. Der Einfluß des eingeblasenen Brennstoffs auf die Strömungsstruktur in einer Überschallbrennkammer wurde mit berührungslosen optischen Meßsystemen untersucht. In diesem Zusammenhang wurde der Einfluß der Brennstoffeinblasung auf die Wiederanlegelänge der freien turbulenten Scherschicht und die Struktur des Stoßsystems nachgewiesen. Der Mischungsprozeß in Überschallbrennkammern wird durch Wirbelstrukturen, die durch lokale Geschwindigkeitsänderungen hervorgerufen wurden, unterstützt [1]. Diese Geschwindigkeitsgradienten erzeugen Verdichtungsstöße, Verdünnungswellen und freie turbulente Scherschichten, die wiederum zu lokalen Dichtegradienten führen. Für die Berechnung der Dichte- und Machzahlverteilung in einer Überschallbrennkammer wurde ein Eulerprogramm verwendet. Die Ergebnisse aus den numerischen Berechnungen wurden zur qualitativen Beschreibung der in den Experimenten nachgewiesenen Strömungsstrukturen eingesetzt.

List of symbols

A_e	entrance cross section
e	specific internal energy
E	total energy
I	intensity of the light beam
M	Mach number
$\dot{m}_{Air}$	mass flow of the main air stream
$\dot{m}_{H_2}$	mass flow of the injected hydrogren
$\dot{m}_{He}$	mass flow of the injected helium
T_0	total temperature of the air
u_i	velocity of the component i
x	coordinate in the flow field
y	coordinate in the flow field
ρ	density
γ	ratio of specific heats

Received April 6, 1994/revised version September 15, 1994

1 Introduction

Reducing the length of combustion chambers and obtaining higher fuel efficiencies of high speed propulsion systems can only be achieved by a better understanding of the complex fuel/air interactions during its mixing. To gain more insight, experimental and numerical data in supersonic flows are needed to investigate the mixing processes [2].

Many previous studies are concerned with the investigation of the flow field in the mixing area of supersonic combustion chambers with different injector systems. Oschwald et al. [3] analysed the flow field of a supersonic combustion chamber in which H_2 is injected through a strut. Schetz et al. [4] analytically investigated the structure of gaseous jets which are injected through holes in the combustion chamber wall into a supersonic stream. Inoue et al. [5] simulated a helium jet, that was transversely injected into a hypersonic flow. The computed flow field show three recirculation zones, the separation shock and the bow shock.

These papers revealed, that shear layers and expansion fans induced by backward facing steps or struts, support the mixing process to obtain fine scale mixing and conditions of flame stability. This work intends to provide data about the structures in the supersonic flow field induced by the fuel injection using a staged fuel injection with a cascade of backward facing steps. In the following chapter of this paper the supersonic wind tunnel with the multistep combustor is described. The chamber walls of the combustor were equipped with windows to enable the application of non-intrusive optical measurement techniques. The third chapter deals with the experimental results obtained by the expansion around a backward facing step with and without injecting helium into the supersonic flow field. These results are monitored by means of shadowgraph technique to obtain qualitative measurements about the gradients in the supersonic flow. Numerical simulations presented in chapter four provide qualitative results concerning the flow structures showing the density and Mach number distribution in the flow field.

2 Experimental setup

The investigation of the mixing process were performed in a supersonic blow down wind tunnel using various geometri-

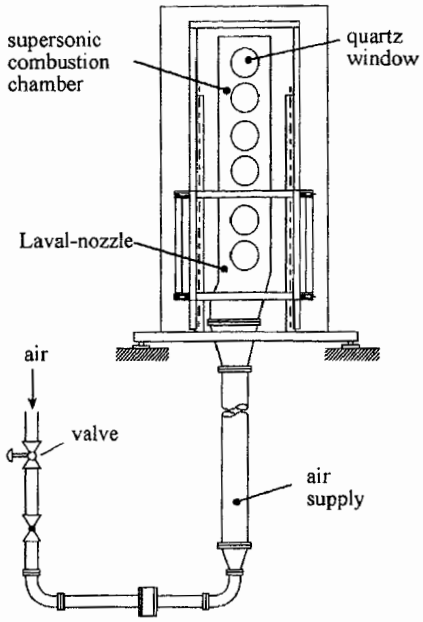

Fig. 1. Supersonic wind tunnel

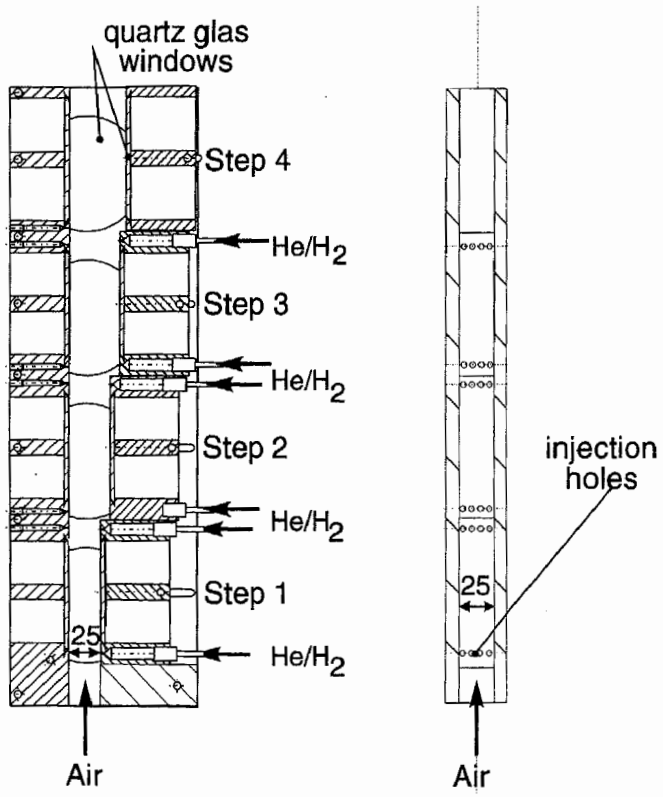

Fig. 2. Multistep combustor

cal configurations for fuel injection. This blowdown wind tunnel with a entrance cross section of A_e=25×25 mm enabled a maximum air Mach number of 2.0 at the inflow. Figure 1 shows a sketch of the wind tunnel and the gas supply system.

This wind tunnel consists of a Laval-contour and a multistep combustion chamber. Along the Laval contour the main airflow is accelerated up to Mach number 2.0±0.1. The total temperature T_0 of the airstream was 293±20 K and the mass flow of the air was $\dot{m}_{Air}$=850 g/s. Downstream of the Laval-nozzel, helium was injected through lines of injection holes mounted in steps 1–3. The mass flow of the injecting helium was varied from $\dot{m}_{He}$=0 to 10 g/s. In the multistep combustor series of downstream rearward facing steps were used to generate large scale turbulent structures in order to obtain

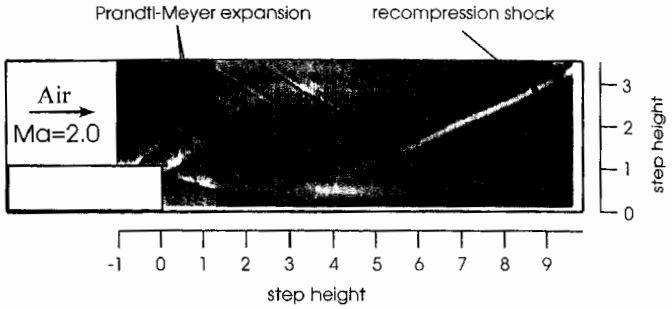

Fig. 3. Supersonic flow over a backward facing step monitored by means of shadowgraph technique

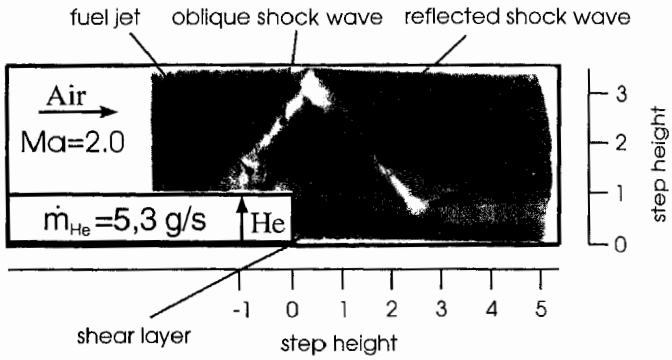

Fig. 4. Supersonic flow field with helium injection ($\dot{m}_{He}$=5,3 $\frac{g}{s}$)

fine-scale mixing through dissipation processes and enhancement of flame stability. The chamber walls were equipped with quartz glass windows to enable the access of optical measurement techniques (Raman Spectroscopy, Laser induced Fluorescence, and shadowgraph technique). Figure 2 shows a sketch of the multistep combustor.

3
Experimental results and discussion

3.1
Supersonic flow over a backward facing step without fuel injection

Basic features of the supersonic flow over a backward-facing step without fuel injection are shown in the shadowgraph in Fig. 3. This figure depicts the Prandtl–Meyer expansion as a v-shaped structure after the corner. A recompression shock forms the reattachment point of the free shear layer, because of the change in the flow direction after the backward facing step. A second oblique shock wave is caused by the reflection of the recompression shock wave on the upper combustion chamber wall. Figure 3 also illustrates that disturbances produced by the wall, have little influence on the other dominating effects like the Prandtl–Meyer expansion and the recompression shock.

3.2
Supersonic flow over a backward facing step with fuel injection

In order to investigate the influence of the injected helium on the supersonic flow structure, the flow field in the mixing area of the first step was observed by means of shadowgraph technique. The stagnation pressure of helium was varied between 3 and 5 bar and the corresponding mass flow was between 5 and 10 g/s. Figures 4, 5 and 6 show the influence of the injected helium on the supersonic flow field. Upstream of the injected fuel jet a oblique shock wave was

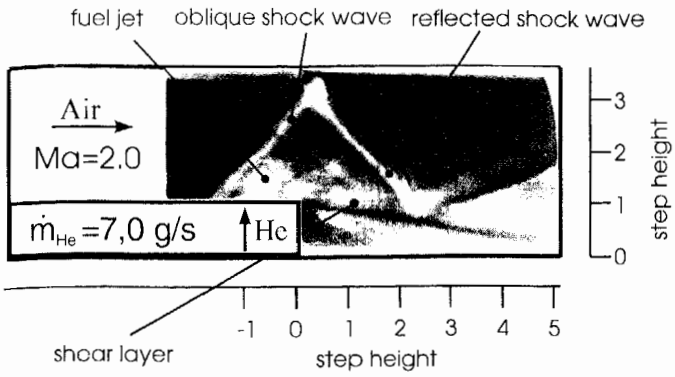

Fig. 5. Supersonic flow field with helium injection ($\dot{m}_{He}=7{,}0\,\frac{g}{s}$)

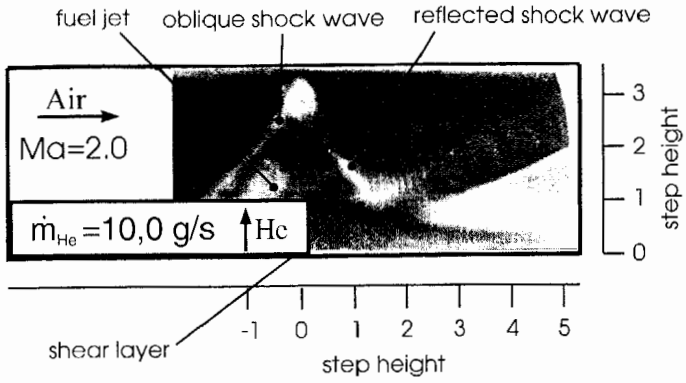

Fig. 6. Supersonic flow field with helium injection ($\dot{m}_{He}=10{,}0\,\frac{g}{s}$)

generated. This shock wave is reflected on the upper chamber wall and impinges onto the mixing shear layer. Comparing figure 4 with figure 3 it can be seen that the reattachment point of the expansion, that is related to the shear layer and the recompression shock wave shifted downstream, when helium was injected. Figures 4, 5 and 6 also show the structure of the mixing layer and its broadening width with increasing the helium mass flux. Increasing helium mass flow rate caused the reflected shock wave to be shifted further upstream and the mixing jet become broader. To reduce the thermal stress of the combustion chamber walls, it is vital to know the reattachment length of the free shear layer.

4
Euler computations of supersonic flow over a backward facing step with helium-injection

4.1
Assumptions and the numerical method

As an aid for interpreting the experimental results of the shadowgraphs we computed a stationary Euler solution of the problem. Although the computation is laminar, large features of the flow are well represented by the non-viscous equations. The time-dependent Euler equations for a compressible fluid are solved using a TVD scheme based on the PPM algorithm by Woodward [6]. It is of fourth order in space in smooth regions of the flow and supposed to be second order near discontinuities. We use Strang's dimension splitting for the extension of the algorithm to two dimensions. This leads to a second order time integration. The governing equations describe the conservation of mass, momentum and energy. The corresponding variables being the density ρ, the components of momentum $\rho \cdot u_i$ and the total energy $E=\rho(e+\frac{1}{2}u_i u_i)$, which are non-dimensionalized by

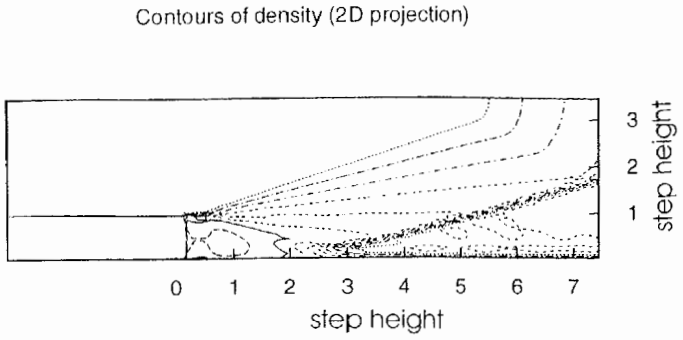

Fig. 7. Contours of density of the case of air flow around a backward facing step on a 20×35 grid. Note the Prandtl–Meyer expansion with the upper angle being the value of the laminar analytical value [8]

reference values given at the inflow. In all computations a perfect diatomic gas with constant specific heat is assumed with a ratio of specific heats to be $\gamma=7/5$. Boundary conditions are supersonic at the $M=2$ inflow and constant extrapolation is used at the outflow. On the walls only the wall normal component of the velocity is set to zero, the other components are linear extrapolated into the wall. The helium is being modelled assuming a γ of 5/3 at the inflow on top of the step to compute the velocity, density and pressure at these points. He-outflow velocity is calculated from the experimental shock angle deflection assuming laminar non-viscous flow. Constant total temperature assumption in the helium pipes leads to the temperature of the outflowing gas. With the experimental mass flux the density can be computed at the outflow and consequently the pressure. The computation is two-dimensional. Mass flux through the holes is small and is about 2% of the mass flux of air at the inflow. From this we conclude, that the approximation of helium as air with low density at the step outflow is a good one. Although no turbulence is involved in the computation we believe that all basic features, e.g. the identification of shocks, are described very well.

4.2
Comparing experiment and computation

4.2.1
Expansion around a backward facing step

Figure 7 shows a computation of the supersonic flow around the backward facing step on a 120×35 grid. The geometry is nondimensionalized with the height of the step in the experimental setup. The Prandtl–Meyer expansion with an upper angle of 30° matches the theoretical value. The lower angle differs from analytical results because of the influence of the lower wall. The Prandtl–Meyer expansion without walls would lead to a Mach number of 20 on the lower branch, while the computation leads to a maximum Mach number of 3.6. One can also see very clearly the recompression shock starting to emanate two step heights downstream of the step, which is in good agreement with the experiment (see Fig. 3). This shock is necessary for changing the flow direction in supersonic flows. Density is lowest in the recirculation zone of the corner with a value of approximately 8% of the inflow density. Figure 8 shows the Mach number distribution. It is evident that the region of subsonic flow is very small and restricted to the area in the corner with a length of about on step height. A comparison of an experimental and the numerical shadowgraph in Figs. 3 and 9 gives a clue of the agreement of numerics and experiment. The numerical shadowgraph was computed using the relation for the

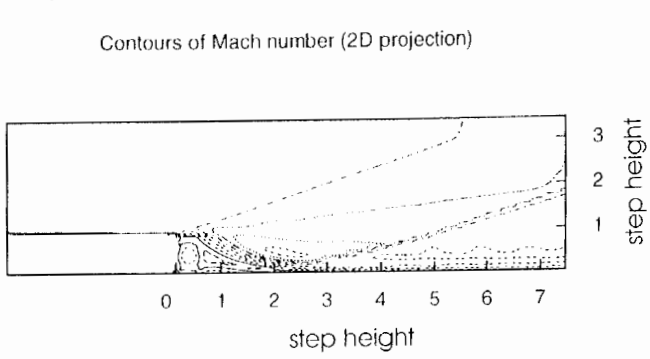

Fig. 8. Contours of Mach number of the case of air flow around a backward facing step on a 20×35 grid. Dashed lines denote subsonic flow regimes. Symbol x denotes the region of maximum Mach number

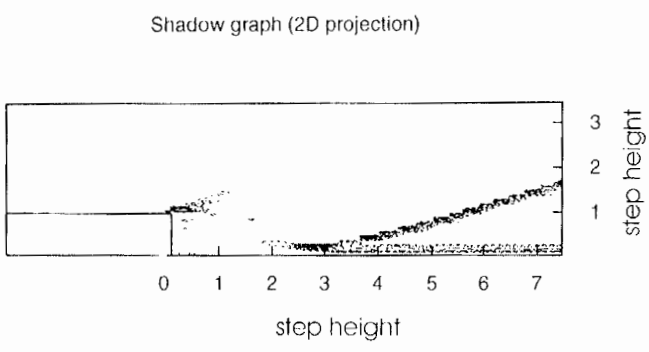

Fig. 9. "Shadowgraph" of the case of air flow around a backward facing step on a 20×35 grid

relative intensity I of the light beam on the fotographic plate [7].

$$\frac{\Delta I}{I} \approx \frac{\partial^2 \rho}{\partial x^2} + \frac{\partial^2 \rho}{\partial y^2}$$

The Mach lines that limit the Prandtl–Meyer expansion in the experiment can be seen, although weakly in the numerics. The recompression shock on the other hand can clearly be observed. We conclude that, although crude approximations were made, basic features of the flow can be identified.

4.2.2
He-injection on a backward facing step

The injection of Helium at a position of about 2/3 of the total step length is modelled by a low density air inflow. Figure 10 shows the density distribution in the flow field with an injected helium mass flux of 5.3 g/s. The shock curvature on the step is due to the supersonic flow up to the inflow. In the experiment, the flow close to the wall is subsonic due to the noslip condition on the wall. Information travels upstream to change the appearance of the shock. The shock is then reflected on the upper wall and interacts with the low density regime about two to three step heights downstream of the step. This is in exellent agreement with the experiment (Fig. 4). Comparing positions of the recompression shock one realizes that it is shifted further downstream with respect to the pure expansion flow case. Decreasing the outflow pressure (not shown) shifts the reflected shock further downstream such it meets the recompression shock with the regime of low density being reduced. Increasing it leads to the same observations of the experiment, i.e. a shift of the reflected shock towards the step. Note that the low density regime is basically confined to the area behind the step and to the vicinity of the wall further downstream. The gradient towards the region of higher density is thereby very steep. In this computation, naturally, nothing can be said about the mixing rate of the two "densities" involved. Maximum value of the density occurs at the upper wall at the reflection point. Looking at the Mach number distribution of Fig. 11 it is evident, that the subsonic regime is elongated with respect to the flow without injection. In the region of the reflected shock interaction zone it is curved outwards and thickened. The outflow itself is subsonic. Maximum Mach number is 2.4 and is reached near the exit. Concerning the size of the subsonic regime it is noteable to say, that the flow near the wall remains subsonic until almost six step heights downstream. The "shadowgraph" of Fig. 12 again is a good representation of the experimental graph. The position of the reflected shock on the upper wall as well as on the low density regime depends – as in the experiment – on the outflow pressure. 5 Discussion and conclusions

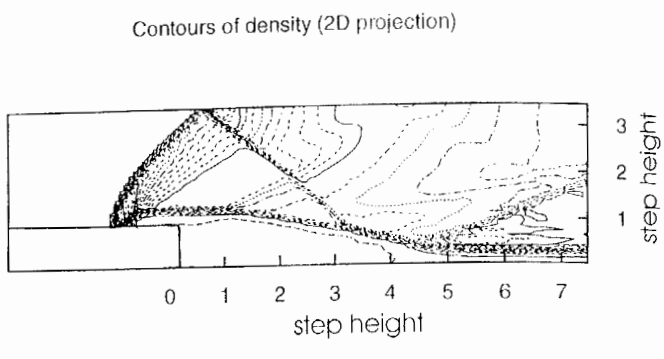

Fig. 10. Contours of density of the case of helium injection on the step on a 20×35 grid. Symbol+denotes region of minimum density

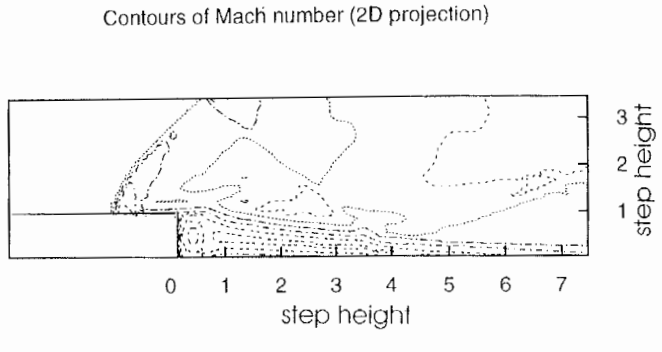

Fig. 11. Contours of Mach number of the helium injection case on the step on a 20×35 grid. Dashed lines denote subsonic flow regimes. Symbol x denotes the region of maximum Mach number

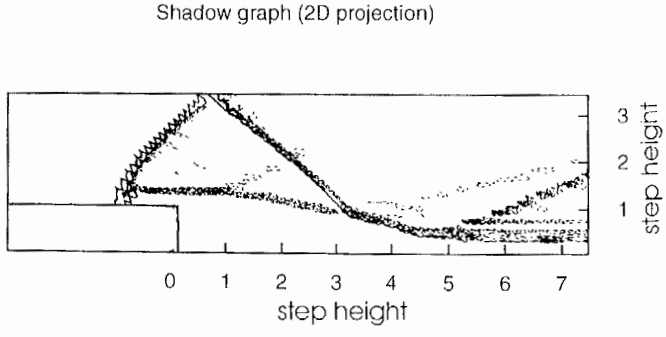

Fig. 12. "Shadowgraph" of the helium injection case on the step on a 20×35 grid. Dashed lines indicate regions of high light intensity, solid lines those of low light intensity

The supersonic flow field with and without fuel injection was studied using numerical and experimental methods. To compute the influence of the injected fuel on the supersonic

flow field an Euler code was used to compute the density and Mach number distribution in the mixing area of the combustion chamber. Although mimicing a viscous flow using an Euler solution does not seem appropriate it still gives a good clue of the flow. The supersonic flow was studied experimentally by using a non-intrusive measurement technique. Especially the influence of the injected fuel mass flow on the structure of the flow field in the mixing area of the combustion chamber was investigated.

Comparison of the Euler code and the experimental results with respect to large scale flow structures shows a very good agreement. The position of shocks and its points of reflection agree well with the experimental observations. Please note, that this good agreement of experiment and numerics is observed in the density contours. Investigation of the density-velocity correlation [9] in turbulent flows shows that it can be negleted outside of shockwaves and outside a region of approximately two Taylor microscales behind the shock. In this light the numerical results helped understanding the flow but are in no means substitutes for turbulent computations. Although no prediction of mixing rates of turbulent quantities could be made, the numerical results help in understanding the influence of parameter changes an experiment cannot deliver. Informations on flow directions – by means of velocity vectors of the laminar flow – can easily be obtained. Code development for using statistical turbulent models is currently under way.

References

1. **Haibel, M.; Mayinger, F.; Strube, G.:** Application of Non-intrusive Diagnostic Methods in Sub- and Supersonic Hydrogen Air Flames. Third International Symposium on Special Topics in Chemical Propulsion: Non-Intrusive Combustion Diagnostics, Scheveningen, The Netherlands, 10–14 May 1993
2. **Dimotakis, P.E.:** Turbulent Free Shear Layer Mixing and Combustion. Progress in Aeronautics and Aeronauties, Vol 137, pp. 265–340
3. **Oschwald, M.; Guerra, R.; Waidmann, W.:** Investigation of the Flow field of a Scramjet Combustor with Parallel H_2-Injection trough a Strut by Particle Image Displacement. Third International Symposium on Special Topics in Chemical Propulsion: Non-Intrusive Combustion Diagnostics, Scheveningen, The Netherlands, 10–14 May 1993
4. **Schetz, J.; Billig, F.:** Penetration of Gaseous Jets Injected into a Supersonic Stream. J. Spacecraft, Vol. 3; No. 11:1658–1665 November 1966
5. **Inoue, Y.; Hayashi, K.; Fujiwara, T.; Miyake, S.; Katsurahara, T.:** Numerical Analysis of Chemical Reactive Flows around Injection Jet into Hypersonic Flow. Pro. 18. Int. Symp. on Space Technology and Science, Kagoshima, 1992
6. **Woodward, P.; Colella P.:** The numerical simulation of two-dimensional fluid flow with strong shocks. J. Comp. Phys., 54:114–173, 1984
7. **Wuest, W.:** Strömungsmeßtechnik. Vieweg, 1969
8. **Anderson, J.D.:** Modern compressible flow. McGraw Hill Company, 1982
9. **Hannappel, R.:** Direkte numerische Simulation der Wechselwirkung eines Verdichtungsstoßes mit isotroper Turbulenz. Ph. D. Thesis, 1993; TU-München